Geophysical Research Letters

RESEARCH LETTER
10.1029/2020GL087148

Regional MJO Modulation of Northwest Pacific Tropical Cyclones Driven by Multiple Transient Controls

M. D. Fowler[1,2,3] and **M. S. Pritchard**[1]

[1]Department of Earth System Science, University of California, Irvine, CA, USA, [2]Cooperative Institute for Research in the Environmental Sciences, University of Colorado Boulder, Boulder, CO, USA, [3]Physical Sciences Laboratory, NOAA Earth System Research Laboratory, Boulder, CO, USA

Key Points:
- Two flavors of MJO-induced cyclogenesis modulation are found in the Northwest Pacific, created by different processes in opposing phases
- TCs in the South China Sea are highly sensitive to the MJO due to combined influences of MJO-induced thermodynamic and dynamic anomalies
- Anomaly phasing leading to wind speed shutdown enables strong MJO control through SSTs in subregions: germane to climate change analysis

Supporting Information:
- Supporting Information S1

Correspondence to:
M. D. Fowler,
mdfowler@uci.edu

Citation:
Fowler, M. D., & Pritchard, M. S. (2020). Regional MJO modulation of Northwest Pacific tropical cyclones driven by multiple transient controls. *Geophysical Research Letters*, *47*, e2020GL087148. https://doi.org/10.1029/2020GL087148

Received 22 JAN 2020
Accepted 11 MAY 2020

Abstract The Madden–Julian Oscillation (MJO) is widely acknowledged for its ability to modulate Northwest Pacific tropical cyclones (TCs), but a complete understanding of the underlying mechanisms remains uncertain. Beyond established effects of the MJO's relative humidity envelope, other dynamical factors have recently been invoked via new genesis potential indices and high-resolution modeling studies. Here we revisit the ability of the MJO to modulate West Pacific TCs through a quasi-explicit cyclone downscaling strategy driven by composited observations, paired later with a genesis index to investigate regional drivers of modulation. We reveal two distinct spatial modes of TC modulation in which the MJO's dynamic and thermodynamic effects act in tandem to increase TCs. In the South China Sea, for instance, shear reductions associated with the MJO's circulation lead to increasing potential intensity ahead of the arrival of a positive humidity anomaly, all of which combine for an extended period of cyclogenesis favorability.

Plain Language Summary Society is bracing for future changes in large-scale tropical weather patterns and especially extremes like tropical cyclones. But before we can hope to understand how these storms will change in the future, we must first understand how and why their formation varies with tropical weather today. The Northwest Pacific in particular is home to more of these storms annually than any other basin, but slow-moving atmospheric patterns that modulate tropical cyclone formations there act in ways that remain to be fully understood. Here, we combine observations with a new downscaling strategy to reveal two distinct patterns of tropical cyclone modulation by an important tropical oscillation, the Madden–Julian Oscillation (MJO). The MJO has already been linked to Northwest Pacific cyclone formation in the past, but the mechanisms are in debate. We suggest that cyclogenesis in the South China Sea is particularly sensitive to the MJO, not just due its historically recognized humidity envelope but rather from a gradual progression of both dynamic and thermodynamic variables associated with this tropical oscillation's complex propagation pattern. This discovery will be important for understanding the effects of climate change on extremes, since the MJO itself is projected to intensify in coming decades.

1. Introduction

Understanding how slow modes of tropical weather modulate tropical cyclone (TC) activity is critical to disaster preparedness. This is especially true in the West Pacific, home to more TCs than any other basin (Ramsay, 2017; H. Zhao et al., 2015) and to the Madden–Julian Oscillation (MJO), a slow-moving (30–60 days) tropical wave that can alter cyclogenesis by modifying large-scale environmental factors like relative humidity and vertical wind shear (Frank & Roundy, 2006; Wu & Takahashi, 2018; C. Zhao & Li, 2018). The MJO is projected to amplify significantly in the future by state-of-the-art climate models (Adames et al., 2017; Arnold et al., 2014, 2015; Maloney et al., 2019) with as yet uncertain consequences for cyclogenesis. Before attempting to understand how the relationship between TCs and the MJO could change in the future, it is necessary to scrutinize their connection today.

Although the MJO has long been recognized to alter TC formation in the West Pacific (Camargo et al., 2009; Huang et al., 2011; J.-H. Kim et al., 2008; Klotzbach, 2014; Liebmann et al., 1994), there is disagreement as to why. Early studies invoked the oscillation's dynamic effects, via wind shear or vorticity anomalies (Hall et al., 2001; Liebmann et al., 1994; Maloney et al., 2000). A landmark study by Camargo et al. (2009) shifted this paradigm to focus instead on the thermodynamic effects of the MJO based on their decomposition of the

Genesis Potential Index (GPI) (Emanuel & Nolan, 2004), arguing for the dominant role of the MJO's humidity envelope. This control-by-humidity argument (with varying degrees of secondary vorticity support) has prevailed in many recent attempts to test causality through analogous GPI decompositions (Huang et al., 2011; You et al., 2018; C. Zhao & Li, 2018; H. Zhao et al., 2015; H. Zhao, Yoshida, & Raga, 2015).

However, there are reasons to think that the situation may yet be more complex. Several of the above studies have been challenged for their reliance on GPI as a sole measure of MJO modulation, which exhibits known biases relative to observations (Bruyère et al., 2012; Camargo et al., 2009; Tippett et al., 2011). Wang and Moon (2017) and Moon et al. (2018) argue that since GPI is tuned to climatology, it may be suboptimal for accurately capturing intraseasonal TC variability associated with the MJO. An alternative intraseasonal genesis index for the West Pacific (Moon et al., 2018) joins with high-resolution modeling experiments (D. Kim et al., 2014; Oouchi et al., 2009) in arguing for renewed attention to dynamical factors of the MJO for modulating cyclogenesis.

One source of disagreement in the above studies is the necessary use of subjective analysis choices to isolate the MJO's influence, through spatial aggregation and smoothing in space-time, to help overcome sampling limitations related to the small number of TCs that have formed in subregions of the Northwest Pacific during individual MJO phases (Figure S1 in the supporting information). A symptom of reasonable disagreement on the details of these choices is that the MJO's modulation of TCs appears to be unsatisfyingly sensitive to details of how the MJO itself is defined, at least when aggregated to large (100°E to 180°W) basin-wide scales (Table S1 and Figure S2). Most studies agree that MJO Phases 5–7 are favorable for cyclogenesis, while a large portion of those in Table S1 also note that monsoon trough amplification or interactions with shorter oscillations can play a role in the observed modulation. But a generalization of favorable phases does not hold across all studies. Recent studies show that simply altering how the MJO is defined across reasonable choices of indices can dramatically change which phases are considered favorable for TC formation in the basin (Lee et al., 2020; You et al., 2018). Such methodological issues may yet belie the complexity of how thermodynamic and dynamic effects conspire within certain subregions of the basin to underpin the essence of MJO-TC modulation.

In light of this context (i.e., the surprising sensitivity of Northwest Pacific MJO-TC modulation to MJO definition, the unresolved debate on its controls, critiques of using GPI alone, and the necessary aggregation across spatiotemporal scales to define MJOs and avoid sampling limitations)—the goal of this study is to revisit the landmark investigation of Camargo et al. (2009) with three new twists. First, beyond GPI, we use an independent explicit cyclone downscaling framework that results in thousands of synthetic TC tracks. That is, before decomposing genesis *potential* to infer causality, we assess its validity versus explicit genesis under each phase of the MJO. Second, we impose another test of credibility based on the hypothesis that robust signals of MJO-TC modulation should be mostly insensitive to the choice of MJO index given the ability of the indices to capture similar large-scale patterns. Finally, we avoid most spatial/temporal aggregation, under the hypothesis, that MJO-TC modulation may be a highly nonlinear process that is prone to happening within preferential hot spots via a sequence of factors that might be otherwise obscured. The results that follow will generally confirm these hypotheses and argue that West Pacific MJO-TC modulation in the current climate is not predominately controlled by dynamics or thermodynamics alone but by unsteady transient contributions from both within preferential regions.

2. Data and Methods

We define the MJO based on two commonly used indices: the outgoing longwave radiation (OLR)-only MJO Index (OMI; Kiladis et al., 2014) and the Real-time Multivariate MJO index, RMM (Wheeler & Hendon, 2004). Our working hypothesis is that if the essential geographic structure of wind and humidity anomalies based on those two indices are not radically different at relatively large scales (where we consider "radically different" to extend beyond a single-phase offset; confirmed in Figures S2–S4), then neither should resulting derived metrics of MJO-TC interaction. In each case, days with an active MJO are identified when their amplitude meets or exceeds one standardized unit and are included in analysis if they occur in the TC season of June–November (Klotzbach, 2014; R. C. Y. Li & Zhou, 2013) during 1983–2013. Note that intraseasonal oscillations in this season are also referred to as Boreal Summer Intraseasonal Oscillations (BSISOs) to differentiate them from the canonical winter MJO, which does not share the BSISO's

northward/northeastward propagation late in its life cycle. That propagation is captured by OMI, which is designed to respect seasonal changes in intraseasonal variability (Kiladis et al., 2014), but is also present to some degree even in RMM (Figures S2–S4). We focus our attention primarily on OMI for its skillful representation of the boreal summer MJO, using the RMM index as a confidence check on those results.

To create a set of expanded TC statistics that allow us to investigate smaller-scale features of the modulation without bumping into sample size limitations, we use a prognostic TC track and intensity forecast model, developed at the Massachusetts Institute of Technology (MIT) with output from WindRiskTech LLC (http://www.windrisktech.com) (Emanuel et al., 2006). This model has been successfully applied and validated across a broad range of topics, including geographic/seasonal climatology and modulation by ENSO along with TC responses to global warming simulations (Daloz et al., 2015; Emanuel, 2010; Emanuel et al., 2008, 2010; Sobel et al., 2019). It operates by seeding initial disturbances with wind speeds ranging from 9–18 knots as weak warm-core vortices randomly in space and time within a high-resolution atmosphere-ocean coupled framework; storms must reach at least 40 kt to be included in the output of the model. In its default use case, the MIT model is built to ingest monthly averages of environmental variables to delineate the mean annual cycle, which is incompatible with application to faster intraseasonal variations. We thus create separate annual cycle climatologies for each phase of the MJO. That is, we group observed days with an active MJO by their calendar month and phase, resulting in the creation of eight phase-specific annual climatologies (see Text S1 for details).

For each day in the phase-specific climatology, the following environmental variables are retrieved from ERA-Interim Reanalysis (ERA-I; Dee et al., 2011): monthly mean sea surface temperature (SST), atmospheric profiles of temperature and humidity, and daily averages of zonal winds at 850 and 250 hPa. The MIT model uses these conditions to produce a set of 4,000 synthetic TC tracks in the Northwest Pacific for each MJO phase as defined by RMM and OMI. The number of storms considered for each phase of the MJO is thus held constant; we assume here that TCs are equally likely to begin in any phase of the MJO rather than establishing an a priori relationship between phase and genesis. We also do not make any initial filtering choices with regard to large-scale climatological signals such as the El Niño–Southern Oscillation (ENSO), consistent with previous studies and in light of previous work suggesting only a small impact on the MJO's modulation of Northwest Pacific cyclogenesis (Klotzbach & Oliver, 2015). Instead, an insensitivity of our main findings to ENSO subcompositing and seasonality is confirmed a posteriori (section 3 and Text S2).

3. Results

The MIT model's composite statistics reveal two prominent geographic action centers of MJO-TC modulation—one located in the eastern half of the basin (the West-Central Pacific (WCPac); Region 5 in Figure 1) and one in the South China Sea (SCS) region (Region 1 in Figure 1). Both exhibit strong MJO-based modulation of genesis density but at phases. This already suggests a more complex modulation of cyclogenesis than a straightforward northeastward propagation following the MJO's humidity envelope, as might be expected from previous studies (Camargo et al., 2009; Camargo & Wing, 2016; Satoh et al., 2012). Instead, the two action centers here are enhanced independently during opposing phases; the intervening regions experience higher rates of cyclogenesis overall (Figures 1a and 1b) and also more geographically diverse responses to the MJO, even within their subdomains (Figures 1c and 1d). Reassuringly, this result of regional favorability is robust independent of how exactly the MJO is indexed in the driving data (i.e., similar patterns from OMI and RMM outside of a single-phase difference, Figure 1).

A propagation of the MJO's cyclogenesis modulation in directions other than its humidity modulation (straight east then northeastward in later phases) has been previously suggested by Zhao, Yoshida, and Raga (2015) and Huang et al. (2011), who highlight the sensitivity to season as well as prevailing larger-scale patterns. Here, with substantially more TC tracks (albeit synthetic ones), we find that the dominant pattern is better described as a set of two preferred action centers wherein the MJO especially modulates cyclogenesis first in the SCS (Phases 2–5) and then in the WCPac (Phases 1 and 2 and 7 and 8). These regions account for 4–13% and 14–27% of the total Northwest Pacific storm formations in the downscaling, depending on MJO phase.

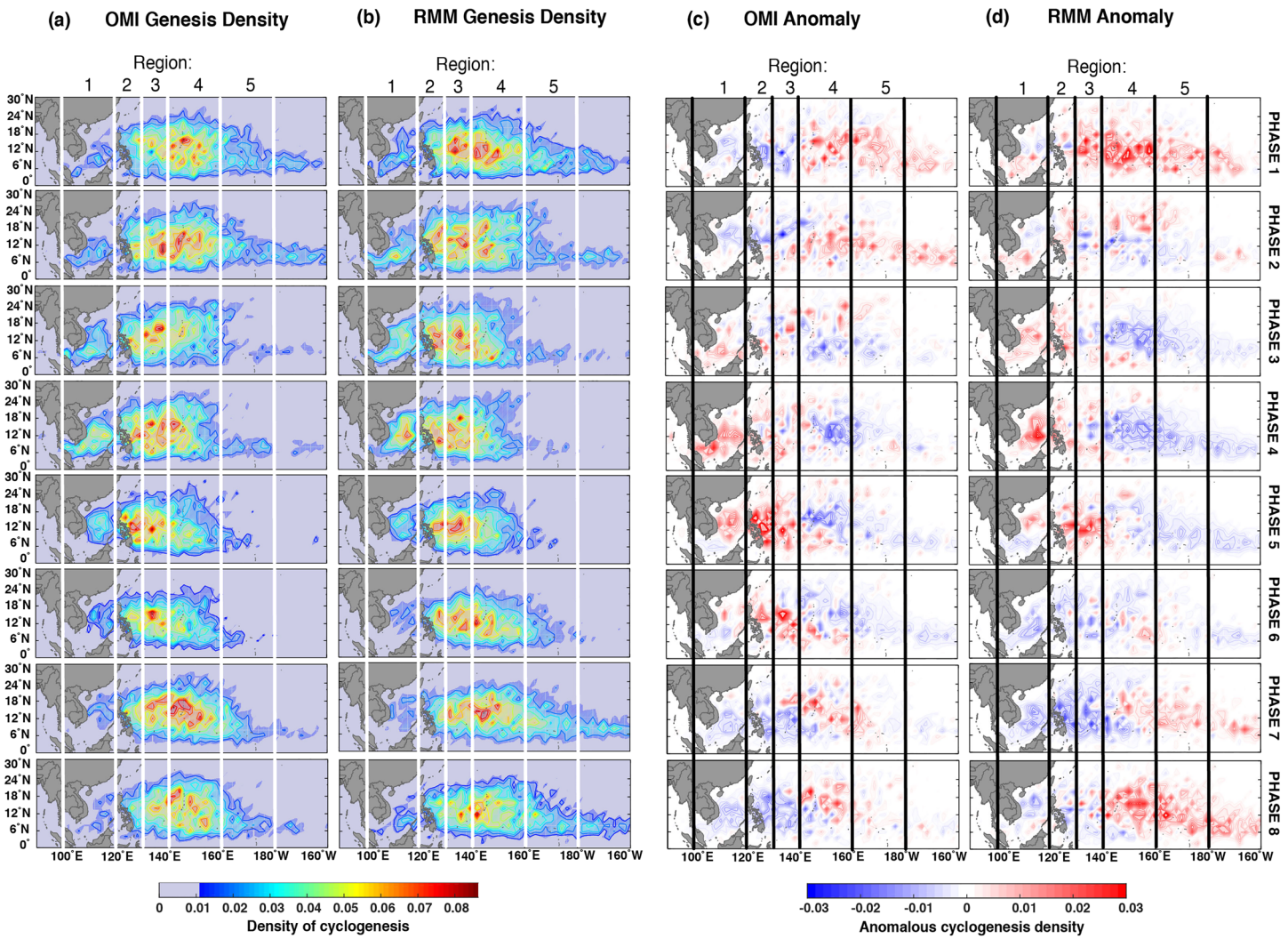

Figure 1. Genesis density (count per degree latitude squared) of MIT model-generated storms in each phase of the MJO as defined by (a) OMI and (b) RMM during the TC season. Anomalies relative to the Phases 1–8 mean of each are shown in (c) and (d), respectively.

Model-based regional sensitivity should ideally be validated against observations, but a direct comparison is hampered by the small number of storms forming in each phase of the MJO on subbasin scales (Figure S1). In Region 5, for instance, no more than five TCs have been observed during any phase of the MJO over the last 40 years. An alternative is to search for similar regional modulations of genesis *potential* using an index such as GPI, which also helps assess causation for this pattern of MJO sensitivity. Though GPI remains one of the most widely used indices for understanding the drivers of TC variability, we acknowledge that it is an imperfect index. Biases in the spatial gradient of cyclogenesis, for example, are readily apparent when compared against either modeled or observed genesis locations (Figure S6). As a result, we constrain our analysis to 5–20°N to limit biases in the northern portion of the basin.

GPI is defined as

$$GPI = \left|10^5 \eta\right|^{\frac{3}{2}} \times \left(\frac{H}{50}\right)^3 \times \left(\frac{V_{pot}}{70}\right)^3 \times (1 + 0.1 V_{shear})^{-2}, \quad (1)$$

where η is the 850 mb absolute vorticity (s^{-1}), H is the 700 hPa relative humidity (%), V_{pot} is the maximum potential intensity (m s^{-1}), and V_{shear} is the vertical wind shear between 850 and 250 mb (m s^{-1}). We estimate it using the same climatology used to drive the MIT model, that is, deriving eight

phase-based climatological annual cycles (at daily resolution) for each of the GPI constituent variables. To determine statistical significance, this is repeated across a 100-member bootstrap ensemble by resampling with replacement. This is repeated to condition the days on ENSO phase, though that record is of course more limited.

To determine the contributions of each term to overall GPI, we follow the established methods of Li et al. (2013) and Zhao and Li (2018) in defining a differential based on the log form of the above equation:

$$\delta GPI = (\delta T1 \times \overline{T2} \times \overline{T3} \times \overline{T4}) + (\delta T2 \times \overline{T1} \times \overline{T3} \times \overline{T4}) + (\delta T3 \times \overline{T1} \times \overline{T2} \times \overline{T4}) + (\delta T4 \times \overline{T1} \times \overline{T2} \times \overline{T3}), \quad (2)$$

where $T1$–$T4$ correspond to each of the four GPI terms, overbars denote the time average over all eight phases of the MJO in June–November within the phase climatology, and δ denotes the phase-specific deviation. The bootstrap ensemble mean GPI anomalies (δGPI) are plotted in Figure 2a for each phase of the MJO and each of the five regions assessed (Figure 2b).

Reassuringly, this GPI analysis reveals a similar pattern of TC modulation relative to the downscaling results (Figure S7). Again, there appear to be two distinct modes of modulation separated into east and west action centers, though the SCS peak is lagged one phase later in GPI compared to the MIT model. In the WCPac (purple curve and bars of Figure 2a), the MJO enhances GPI in Phases 1 and 2 and 7 and 8, indicating an environment that is more favorable for cyclogenesis than during Phases 4–6. The western part of the basin (red, yellow, and green bars in Figure 2a), however, shows the largest positive GPI anomalies in Phases 3–6 instead, suppressing genesis potential in Phases 1 and 2 and 7 and 8. Swapping RMM for OMI as the MJO index does not change these key features of the GPI decomposition beyond a single-phase offset (Figure S8), thus passing our credibility test for a robust subregional signal of MJO-TC modulation. Repeating this analysis after subsampling by season or ENSO phase also produces consistent effects, further reassuring that this is a direct effect of the MJO and not the result of unintended aliasing from longer time scales (Text S2 and Figures S9 and S10).

Despite qualitative agreement between GPI and MIT-modeled cyclogenesis, we recognize that GPI has come under scrutiny for its inability to capture intraseasonal TC variability. Camargo et al. (2009) note that the index captured only 50% of the expected TC modulation on MJO timescales, based on a comparison with GPI's sensitivity to the annual cycle. We carry out a similar analysis here by comparing monthly anomalous GPI and downscaled cyclogenesis with phase anomaly versions of the same plot (Figure S11 and Text S2), assessing each domain individually to avoid the basin-scale inconsistencies illustrated above. Reassuringly, there is a clear connection between GPI and downscaled TCs even when model results are used, with regional sensitivities that are mostly self-consistent across timescales (based on the ordering of regional regression lines in Figure S11). Correlation coefficients between the model and GPI on seasonal timescales range from 0.95–0.99 as expected and remain relatively high for Regions 1 and 5 on MJO timescales as well (0.86 and 0.96, respectively). This exercise also reveals a surprising discrepancy in the *climatological* relationship by region, which suggests that GPI calibration as in Camargo et al. (2009) may also benefit from subbasin analysis.

Under the assumption that GPI is a sufficiently accurate tool for capturing TC variability in the MIT model, we are now equipped to address the main question: Why does the MJO preferentially modulate cyclogenesis in these hot spots? We begin with the SCS since, in the downscaling and especially the GPI analysis, Region 1 stands out as being highly sensitive to MJO phase. It exhibits the largest range of GPI anomalies, and the downscaled genesis density shows one of the largest differences between middle and early/late phases of the MJO in this region as well. But why?

Assessing the individual drivers of GPI and the background winds at upper and lower levels suggests that the SCS region is uniquely situated so as to be highly responsive to both convective and circulation anomalies associated with the MJO (Figures 3a and 3b). Since this region is characterized by weak background low-level winds (blue dashed line in Figure 3a), the arriving sheared circulation anomaly is able to induce a near shutdown of the 850 hPa zonal wind speed magnitude beginning in Phase 2. Reduced winds ahead of (to the east of) the arriving MJO's humidity envelope set the stage for an important ocean interaction, through reduced evaporative cooling, turbulent mixing, and ocean mixed layer depths. These prime the

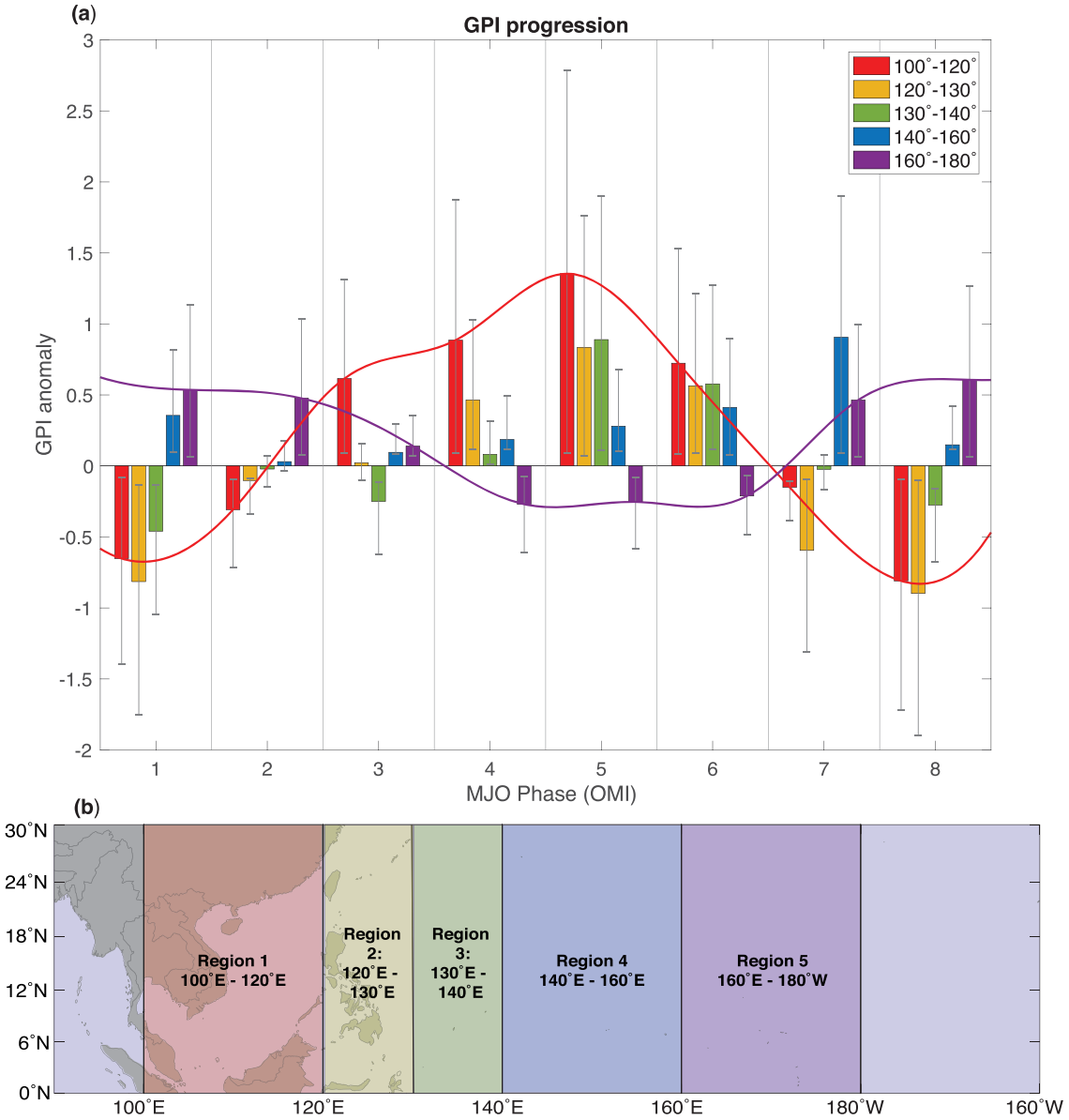

Figure 2. (a) Anomalous GPI for each phase of the OMI-defined MJO relative to the Phases 1–8 mean (equation 2). Each of the five regions outlined in (b) are assessed independently, shown as colored bars in (a), which represent the mean of the 100-member bootstrap for the TC season; error bars correspond to the 25th and 75th percentiles of that analysis. Curves for Regions 1 and 5 are matched to the histogram for ease of comparing the two modes.

pump for a regional positive SST anomaly (Figure S12), especially since ahead of the arrival of the convectively active portion of the MJO, in Phases 1 and 2, a positive OLR anomaly (i.e., less clouds and more incoming surface solar radiation) is present (Figure S3). Together, we interpret these effects as the root cause that ultimately increases potential intensity support for cyclogenesis beginning in Phase 3 (yellow bars in Figures 3b and S12). This succession of increasing GPI support, first from shear and then potential intensity (through wind-speed and subsidence), is followed by the arriving relative humidity anomaly of the MJO in Phase 5, acting to further support and sustain enhanced GPI through Phase 6 (orange bars in Figure 3b). Relative humidity is thus only part of the story—shear and potential intensity are equally important from the vantage point of this especially susceptible region.

The SCS region stands out as having the strongest trifold support from these successive drivers of regional GPI. While Regions 2 and 3 behave similarly in terms of sharing the same canonical GPI support

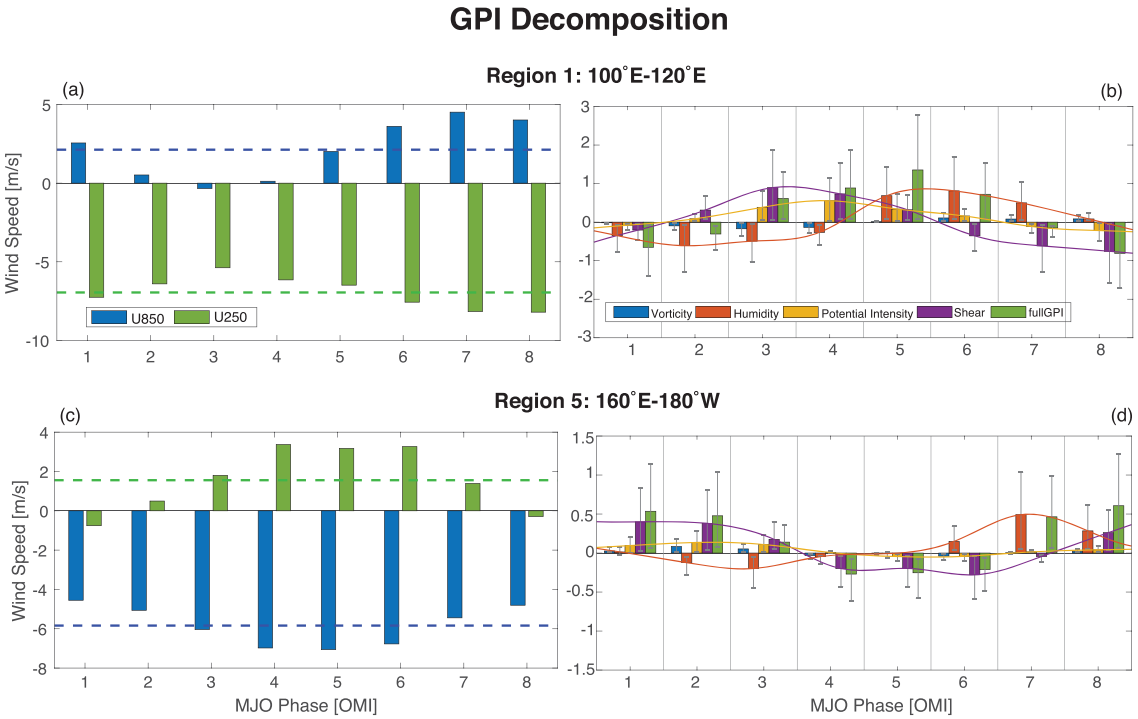

Figure 3. (a, c) Average 850 (blue) and 250 (green) mb winds in the 100-member bootstrap ensemble for each phase of the MJO; dashed lines represent the Phases 1–8 mean. (b, d) Average GPI decomposition (equation 2) for each MJO phase in the bootstrap ensemble. Error bars correspond to the 25th and 75th percentiles. Curves for wind shear (purple), potential intensity (gold), and relative humidity (orange) are fitted to the histograms as in Figure 2 for ease of viewing the transient progression of each variable to overall GPI. Regional averages are taken over 5–20°N in the TC season.

sequence (Figure S13), they do not exhibit nearly as large of a total GPI modulation by the MJO. We infer that the SCS region is special because it is situated geographically at an important location relative to the background Walker Cell, such that the MJO-induced reduction in shear coincides with near-zero low-level wind speeds. Together with clear skies, this supports stronger, more sustained SST anomalies (Figure S12), leading to especially favorable conditions for MJO modulation of cyclogenesis through the potential intensity term, in addition to support from shear and relative humidity.

In contrast, the second geographic action center in the WCPac (Region 5) shows a distinctly different cause of MJO-based GPI modulation (Figure 3d). In a reversal of the previously described pattern, relative humidity increases are now the leading force of increased GPI during Phases 7 and 8 rather than the trailing one. Enhanced favorability for cyclogenesis is then sustained through Phases 1 and 2 by reductions in wind shear due to a reduction/reversal in upper-level winds (Figure 3c). Region 4 exhibits similar phasing—GPI is more heavily favored in the early and late phases of the MJO through similar mechanisms (Figure S13). But as in the case of modeled genesis density, GPI anomalies remain consistently positive there throughout the MJO's life cycle, making it difficult to conclude definitively that the MJO exerts a primary control on cyclogenesis in the region.

4. Discussion and Conclusions

The boreal summer MJO has often been noted for its ability to modulate Northwest Pacific cyclogenesis (Camargo et al., 2009; Huang et al., 2011; J.-H. Kim et al., 2008; Klotzbach, 2014; Liebmann et al., 1994). But disagreement on the drivers of that modulation, small TC sample sizes, variability in methods of aggregation, and questions about the limitations of GPI have all limited robust conclusions about the underlying processes and their geographic details. Here, we have revisited the issue with a quasi-explicit TC downscaling framework and multiple MJO index credibility testing to identify robust subregional action centers, paired later with GPI to understand their causality.

Our results are at odds with the paradigm that the MJO primarily influences cyclogenesis through relative humidity support in ways that mostly propagate with its convective core (Camargo et al., 2009; Camargo & Wing, 2016; Satoh et al., 2012). Instead, genesis density from the MIT model indicates a more complicated pattern of modulation in which distinct geographic action centers within the basin respond disproportionately to the passage of the MJO and for different reasons. Two particular hot spots are modulated out of phase with one another, with the West-Central Pacific most active during Phases 1 and 2 and 7 and 8, while the South China Sea is favored during Phases 3–5.

In hindsight, these two preferred action centers are visible in previous studies as well. The phasing of the SCS favorability is roughly consistent with (though a bit earlier than) Camargo et al. (2009) (their Figure 4) and Huang et al. (2011) (their Figure 8), where close inspection also shows hints of a WCPac favorability region toward the beginning/end of the MJO life cycle. Kim et al. (2014), in a high-resolution modeling study, found that increases in SCS cyclogenesis began in Phases 3 + 4, also in line with our results.

The SCS region stands out in our analysis as uniquely prone to MJO-driven TC modulation. Cyclogenesis there is strongly enhanced during the middle of the MJO's life cycle via a reduced shear packet that precedes the convective anomaly. Due to favorable background low-level winds, this locally increases SSTs, presumably due to strong interactions with surface ocean heat content linked to both wind-induced surface flux shutdown (and thermocline shoaling) as well as clear skies ahead of the convection. The resulting increase in potential intensity, though rarely emphasized as a critical factor in previous studies, helps sustain positive GPI anomalies throughout Regions 1–3 before yielding to humidity support. This happy coincidence of three successive avenues of support for cyclogenesis is unique to the far western part of the basin and may explain why the decks are stacked there for an especially strong MJO modulation.

Some limitations of this study are important to note. The GPI approach, as suggested previously, suffers from its own biases despite qualitative agreement with our downscaling. Tippett et al. (2011), for example, note that GPI may be enhanced even in regions or seasons when TCs are not observed; such bias relative to observations is confirmed independently here. There is also reason to suspect that GPI may not fully capture the intraseasonal variability of cyclogenesis (Camargo et al., 2009; Moon et al., 2018; Wang & Moon, 2017), which could argue for the avoidance of such an index altogether. Despite this possibility, we show that MIT modeled TC counts maintain reasonably high levels of agreement with GPI when they are considered on seasonal as well as intraseasonal timescales; combined with the widespread acceptance of GPI in previous TC studies, we feel it is a reasonable first estimate of the mechanisms driving MJO-TC modulation. A significant priority for future work, however, should focus on independent verification of TC sensitivity to each driver, potentially via a series of modeling experiments wherein environmental factors are changed in isolation to determine phase-based controls on cyclogenesis. A related systematic limitation on our results is temporal aggregation—we have intentionally aggregated data based on MJO phase and without regard for other environmental signals and their nonlinear interactions, a practical necessary to avoid excessive computational costs and employ a state-of-the-art downscaling technique built around monthly averages.

If a similarly efficient, high-performing downscaling technique emerges that can yield large TC samples using daily observations that *could* respect such interactions, this work points to what could be an important approach to consider when interpreting results: hunting for interactions that promote shutdowns of near-surface wind speeds and subsequent potential intensity feedbacks that precede the arrival of the MJO's convective envelope. We have proven through multiple indices and analytical approaches that such interactions appear to cause regions of the Northwest Pacific to be anomalously sensitive to the passage of the MJO with regard to cyclogenesis. These results speak to the importance of further studies employing additional MJO- and TC-resolving models to confirm/refine such subregional sensitivity.

This may be particularly crucial to consider in light of the fact that numerous studies now suggest MJO amplification as a result of climate change (Adames et al., 2017; Arnold et al., 2014, 2015; Maloney et al., 2019). Modern climate models including prototypes with explicit convection suggest that this amplification could include precipitation intensification (Arnold et al., 2014; Chang et al., 2015; Maloney et al., 2019) as well as changes in the efficiency with which convective heating is converted into wind anomalies (Wolding et al., 2017). MJO events may also become more frequent, propagate faster, and expand further eastward (Adames et al., 2017; Arnold et al., 2014; Maloney et al., 2019). That expansion could feasibly reach into the western hot spot of modulation highlighted in the MIT model and even more strongly in GPI.

Though only a few storms have formed in this region to date, an extension may allow the MJO modulation to project more clearly onto observations in the coming decades. Future studies on the consequences of MJO amplification on cyclogenesis in the Northwest Pacific will thus likely benefit not only from considering the nonlinear temporal interactions between changing oscillation characteristics, mean states, and other tropical waves but also from searching for where the combination of those changes conspire to produce sustained surface wind shutdowns capable of similarly strong feedbacks.

Data Availability Statement

The data analyzed from the MIT model was produced by WindRiskTech LLC, with whom the authors have a signed data license agreement not to personally publish/transmit/transfer the proprietary data. The downscaled data can, however, be made available upon individual requests for research purposes from Prof. Kerry Emanuel, the Chief Scientific Officer of WindRiskTech (emanuel@mit.edu). A series of analysis code not included in Kerry Emanuel's Matlab package are available at https://github.com/megandevlan/TCs-MJO (DOI: 10.5281/zenodo.3620834).

Acknowledgments

This study was conducted with primary funding from the Department of Energy Early Career Program (DE-SC0012152) and additional support from the NSF (AGS-1734164) and NASA MIRO (NNX15AQ06A). We extend our thanks to WindRiskTech LLC and Kerry Emanuel for his generation of the downscaling results and for helpful conversations regarding this work. The authors also thank Jim Randerson and Tom Beucler for helpful suggestions that helped improve the manuscript.

References

Adames, A. F., Kim, D., Sobel, A. H., Del Genio, A., & Wu, J. (2017). Changes in the structure and propagation of the MJO with increasing CO_2. *Journal of Advances in Modeling Earth Systems*, *9*(2), 1251–1268. https://doi.org/10.1002/2017MS000913

Arnold, N. P., Branson, M., Burt, M. A., Abbot, D. S., Kuang, Z., Randall, D. A., & Tziperman, E. (2014). Effects of explicit atmospheric convection at high CO_2. *PNAS*, *111*(30), 10943–10948. https://doi.org/10.1073/pnas.1407175111

Arnold, N. P., Branson, M., Kuang, Z., Randall, D. A., & Tziperman, E. (2015). MJO intensification with warming in the superparameterized CESM. *Journal of Climate*, *28*(7), 2706–2724. https://doi.org/10.1175/JCLI-D-14-00494.1

Bruyère, C. L., Holland, G. J., & Towler, E. (2012). Investigating the use of a genesis potential index for tropical cyclones in the North Atlantic basin. *Journal of Climate*, *25*(24), 8611–8626. https://doi.org/10.1175/JCLI-D-11-00619.1

Camargo, S. J., Wheeler, M. C., & Sobel, A. H. (2009). Diagnosis of the MJO modulation of tropical cyclogenesis using an empirical index. *Journal of the Atmospheric Sciences*, *66*(10), 3061–3074. https://doi.org/10.1175/2009JAS3101.1

Camargo, S. J., & Wing, A. A. (2016). Tropical cyclones in climate models. *WIREs Climate Change*, *7*(2), 211–237. https://doi.org/10.1002/wcc.373

Chang, C.-W. J., Tseng, W.-L., Hsu, H.-H., Keenlyside, N., & Tsuang, B.-J. (2015). The Madden–Julian Oscillation in a warmer world. *Geophysical Research Letters*, *42*(14), 6034–6042. https://doi.org/10.1002/2015GL065095

Daloz, A. S., Camargo, S. J., Kossin, J. P., Emanuel, K., Horn, M., Jonas, J. A., et al. (2015). Cluster analysis of downscaled and explicitly simulated North Atlantic tropical cyclone tracks. *Journal of Climate*, *28*(4), 1333–1361. https://doi.org/10.1175/JCLI-D-13-00646.1

Dee, D. P., Uppala, S. M., Simmons, A. J., Berrisford, P., Poli, P., Kobayashi, S., et al. (2011). The ERA-interim reanalysis: Configuration and performance of the data assimilation system. *Quarterly Journal of the Royal Meteorological Society*, *137*(656), 553–597. https://doi.org/10.1002/qj.828

Emanuel, K. (2010). Tropical cyclone activity downscaled from NOAA-CIRES reanalysis, 1908–1958. *Journal of Advances in Modeling Earth Systems*, *2*(1), 1. https://doi.org/10.3894/JAMES.2010.2.1

Emanuel, K., & Nolan, D. S. (2004). Tropical cyclone activity and the global climate system. In 26th Conference on Hurricanes and Tropical Meteorolgy (pp. 240–241). Miami, FL. Retrieved from ftp://texmex.mit.edu/pub/emanuel/PAPERS/em_nolan_extended_2004.pdf

Emanuel, K., Oouchi, K., Satoh, M., Tomita, H., & Yamada, Y. (2010). Comparison of explicitly simulated and downscaled tropical cyclone activity in a high-resolution global climate model. *Journal of Advances in Modeling Earth Systems*, *2*(4), 2. https://doi.org/10.3894/JAMES.2010.2.9

Emanuel, K., Ravela, S., Vivant, E., & Risi, C. (2006). A statistical deterministic approach to hurricane risk assessment. *Bulletin of the American Meteorological Society*, *87*(3), 299–314. https://doi.org/10.1175/BAMS-87-3-299

Emanuel, K., Sundararajan, R., Williams, J., Emanuel, K., Sundararajan, R., & Williams, J. (2008). Hurricanes and global warming: Results from downscaling IPCC AR4 simulations. *Bulletin of the American Meteorological Society*, *89*(3), 347–368. https://doi.org/10.1175/BAMS-89-3-347

Frank, W. M., & Roundy, P. E. (2006). The role of tropical waves in tropical cyclogenesis. *Monthly Weather Review*, *134*(9), 2397–2417. Retrieved from.

Hall, J. D., Matthews, A. J., Karoly, D. J., Hall, J. D., Matthews, A. J., & Karoly, D. J. (2001). The modulation of tropical cyclone activity in the Australian region by the Madden–Julian Oscillation. *Monthly Weather Review*, *129*(12), 2970–2982. https://doi.org/10.1175/1520-0493(2001)129<2970:TMOTCA>2.0.CO;2

Huang, P., Chou, C., & Huang, R. (2011). Seasonal modulation of tropical intraseasonal oscillations on tropical cyclone geneses in the Western North Pacific. *Journal of Climate*, *24*(24), 6339–6352. https://doi.org/10.1175/2011JCLI4200.1

Kiladis, G. N., Dias, J., Straub, K. H., Wheeler, M. C., Tulich, S. N., Kikuchi, K., et al. (2014). A comparison of OLR and circulation-based indices for tracking the MJO. *Monthly Weather Review*, *142*(5), 1697–1715. https://doi.org/10.1175/MWR-D-13-00301.1

Kim, D., Lee, M.-I., Kim, H.-M., Schubert, S. D., & Yoo, J. H. (2014). The modulation of tropical storm activity in the Western North Pacific by the Madden–Julian Oscillation in GEOS-5 AGCM experiments. *Atmospheric Science Letters*, *15*(4), 335–341. https://doi.org/10.1002/asl2.509

Kim, J.-H., Ho, C.-H., Kim, H.-S., Sui, C.-H., & Park, S. K. (2008). Systematic variation of summertime tropical cyclone activity in the Western North Pacific in relation to the Madden–Julian Oscillation. *Journal of Climate*, *21*(6), 1171–1191. https://doi.org/10.1175/2007JCLI1493.1

Klotzbach, P. J. (2014). The Madden–Julian Oscillation's impacts on worldwide tropical cyclone activity. *Journal of Climate*, *27*(6), 2317–2330. https://doi.org/10.1175/JCLI-D-13-00483.1

Klotzbach, P. J., & Oliver, E. C. J. (2015). Variations in global tropical cyclone activity and the Madden-Julian Oscillation since the midtwentieth century. *Geophysical Research Letters*, *42*(10), 4199–4207. https://doi.org/10.1002/2015GL063966

Lee, C.-Y., Camargo, S. J., Vitart, F., Sobel, A. H., Camp, J., Wang, S., et al. (2020). Subseasonal predictions of tropical cyclone occurrence and ACE in the S2S dataset. *Weather and Forecasting*, *35*(3), 921–938. https://doi.org/10.1175/waf-d-19-0217.1

Li, R. C. Y., & Zhou, W. (2013). Modulation of Western North Pacific tropical cyclone activity by the ISO. Part I: Genesis and intensity. *Journal of Climate*, *26*(9), 2904–2918. https://doi.org/10.1175/JCLI-D-12-00210.1

Li, Z., Yu, W., Li, T., Murty, V. S. N., & Tangang, F. (2013). Bimodal character of cyclone climatology in the Bay of Bengal modulated by monsoon seasonal cycle. *Journal of Climate*, *26*(3), 1033–1046. https://doi.org/10.1175/JCLI-D-11-00627.1

Liebmann, B., Hendon, H. H., & Glick, J. D. (1994). The relationship between tropical cyclones of the western Pacific and Indian Oceans and the Madden–Julian Oscillation. *Journal of the Meteorological Society of Japan*, *72*, 401–412. Retrieved from. https://doi.org/10.2151/jmsj1965.72.3_401

Maloney, E. D., Adames, Á. F., & Bui, H. X. (2019). Madden–Julian Oscillation changes under anthropogenic warming. *Nature Climate Change*, *9*(1), 26–33. https://doi.org/10.1038/s41558-018-0331-6

Maloney, E. D., Hartmann, D. L., Maloney, E. D., & Hartmann, D. L. (2000). Modulation of Eastern North Pacific Hurricanes by the Madden–Julian Oscillation. *Journal of Climate*, *13*(9), 1451–1460. https://doi.org/10.1175/1520-0442(2000)013<1451:MOENPH>2.0.CO;2

Moon, J.-Y., Wang, B., Lee, S.-S., & Ha, K.-J. (2018). An intraseasonal genesis potential index for tropical cyclones during northern hemisphere summer. *Journal of Climate*, *31*(22), 9055–9071. https://doi.org/10.1175/JCLI-D-18-0515.1

Oouchi, K., Noda, A. T., Satoh, M., Miura, H., Tomita, H., Nasuno, T., & Iga, S. (2009). A simulated preconditioning of typhoon genesis controlled by a boreal summer Madden–Julian Oscillation event in a global cloud-system-resolving model. *Solaiat*, *5*, 65–68. https://doi.org/10.2151/sola.2009-017

Ramsay, H. (2017). The global climatology of tropical cyclones. In *Oxford research encyclopedia of natural hazard science* (pp. 1–34). USA: Oxford University Press. https://doi.org/10.1093/acrefore/9780199389407.013.79

Satoh, M., Oouchi, K., Nasuno, T., Taniguchi, H., Yamada, Y., Tomita, H., et al. (2012). The intra-seasonal oscillation and its control of tropical cyclones simulated by high-resolution global atmospheric models. *Climate Dynamics*, *39*(9–10), 2185–2206. https://doi.org/10.1007/s00382-011-1235-6

Sobel, A. H., Lee, C.-Y., Camargo, S. J., Mandli, K. T., Emanuel, K. A., Mukhopadhyay, P., & Mahakur, M. (2019). Tropical cyclone hazard to Mumbai in the recent historical climate. *Monthly Weather Review*, *147*(7), 2355–2366. https://doi.org/10.1175/MWR-D-18

Tippett, M. K., Camargo, S. J., & Sobel, A. H. (2011). A Poisson regression index for tropical cyclone genesis and the role of large-scale vorticity in genesis. *Journal of Climate*, *24*(9), 2335–2357. https://doi.org/10.1175/2010JCLI3811.1

Wang, B., & Moon, J.-Y. (2017). An anomalous genesis potential index for MJO modulation of tropical cyclones. *Journal of Climate*, *30*(11), 4021–4035. https://doi.org/10.1175/JCLI-D-16-0749.1

Wheeler, M. C., & Hendon, H. H. (2004). An all-season real-time multivariate MJO index: Development of an index for monitoring and prediction. *Monthly Weather Review*, *132*(8), 1917–1932. https://doi.org/10.1175/1520-0493(2004)132<1917:AARMMI>2.0.CO;2

Wolding, B. O., Maloney, E. D., Henderson, S., & Branson, M. (2017). Climate change and the Madden–Julian Oscillation: A vertically resolved weak temperature gradient analysis. *Journal of Advances in Modeling Earth Systems*, *9*(1), 307–331. https://doi.org/10.1002/2016MS000843

Wu, L., & Takahashi, M. (2018). Contributions of tropical waves to tropical cyclone genesis over the western North Pacific. *Climate Dynamics*, *50*(11–12), 4635–4649. https://doi.org/10.1007/s00382-017-3895-3

You, L., Gao, J., Lin, H., & Chen, S. (2018). Impact of the intra-seasonal oscillation on tropical cyclone genesis over the western North Pacific. *International Journal of Climatology*, *39*(4), 1969–1984. https://doi.org/10.1002/joc.5927

Zhao, C., & Li, T. (2018). Basin dependence of the MJO modulating tropical cyclone genesis. *Climate Dynamics*, *52*(9-10), 6081–6096. https://doi.org/10.1007/s00382-018-4502-y

Zhao, H., Jiang, X., & Wu, L. (2015). Modulation of Northwest Pacific tropical cyclone genesis by the intraseasonal variability. *Journal of the Meteorological Society of Japan*, *93*(1), 81–97. https://doi.org/10.2151/jmsj.2015-006

Zhao, H., Yoshida, R., & Raga, G. B. (2015). Impact of the Madden–Julian Oscillation on Western North Pacific tropical cyclogenesis associated with large-scale patterns. *Journal of Applied Meteorology and Climatology*, *54*(7), 1413–1429. https://doi.org/10.1175/JAMC-D-14-0254.1